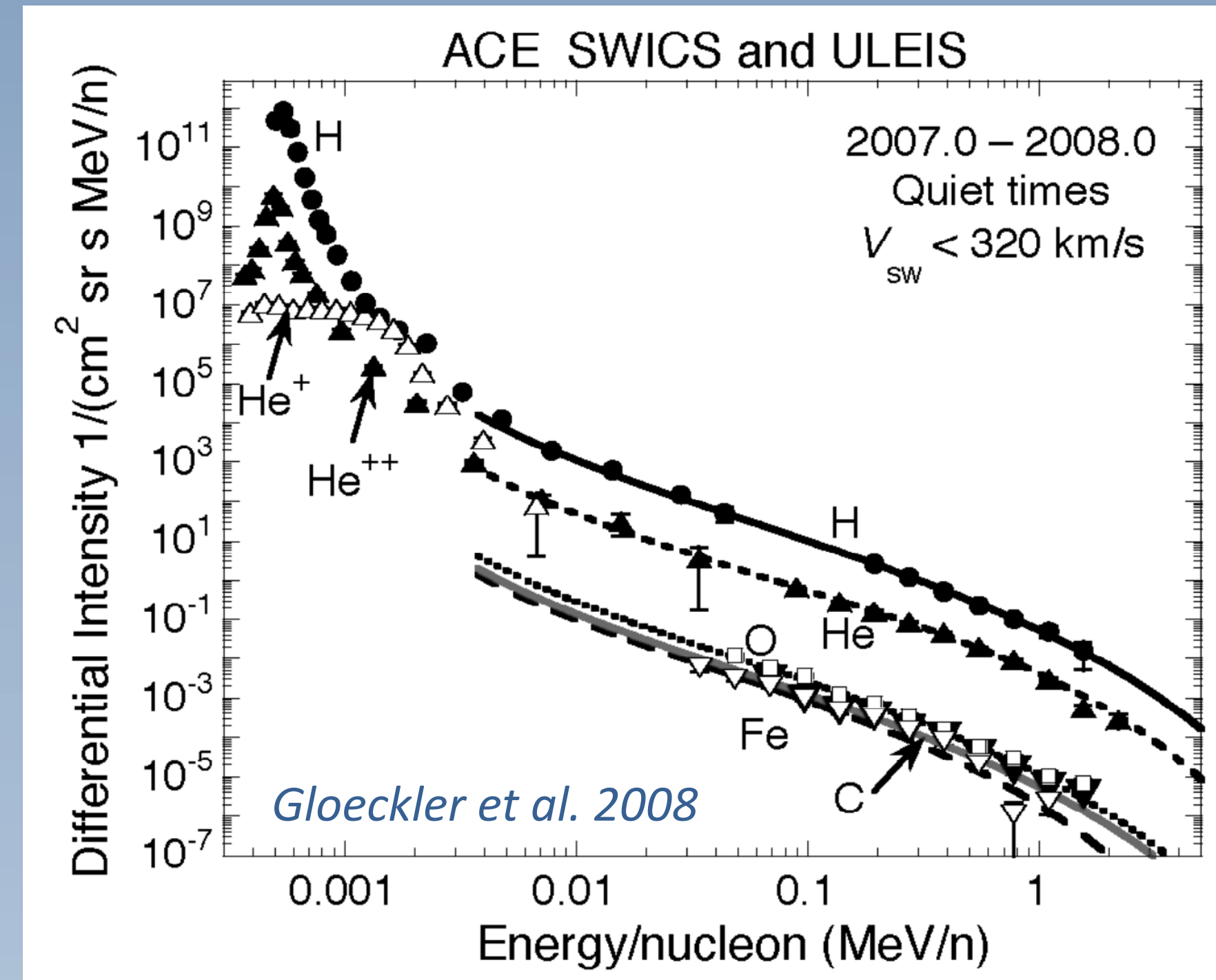


## Introduction

The presence of suprathermal tails in interplanetary space even during quiet times, as selected by pre-defined Solar Wind (SW) speed threshold [1, 3] (Fig. 1) or energetic and suprathermal particle rate threshold [2], was first pointed out by Gloeckler et al. [3] and led to ample follow-up work. They demonstrated that the spectra exhibit a constant  $v^{-5}$  slope and suggested that tails are present everywhere and all the time. They extended the spectral description with an exponential term accounting for losses at high energies due to finite space and time [1]. Later the composition of the suprathermal ions and the spectra of heavier species was studied systematically [4, 5], revealing variability of the heavy ion spectra and, in particular, variation with the solar cycle.



**FIGURE 1:** Suprathermal tails of H through Fe, observed with ACE SWICS and ULEIS during Quiet Times as defined by a solar wind speed threshold [1].

## Models for Suprathermal Tails

Two different types of models have been developed to explain the observed suprathermal tail populations:

- Continuous local acceleration in undisturbed SW
- Acceleration in and leakage from compressions or shocks of coronal mass ejection (CME) and stream interaction regions (SIR).
- The former inspired by the widely promoted constant power law and presence during quiet times:
- Suggested is compressional turbulence in the SW [2, 6, 7] to naturally provide a  $v^{-5}$  spectrum. But there are weaknesses in the derivation [8].
- Wave particle interaction [9] and stochastic acceleration [10] produce spectra close to  $v^{-5}$ , with adiabatic cooling included.
- The latter come in various forms:
- Reconnection in distributed magnetic islands produces Mach number dependent power laws, towards  $v^{-5}$  in the outer heliosphere [11, 12], strongest downstream of shocks [13].
- Shock and compressional acceleration at SIR and CME produce Mach number dependent power laws [14, 15, 16].
- Transit time damping acceleration in SIRs leads to indices -5 to -6, with lower efficiency in quiet SW [17], thus may be a hybrid model.

## Localized or Distributed Source of Tails?

This dichotomy raises the question: Does the strength and shape of tails vary with distance from a localized source or not?

Concentrating on tails within compressions, a strong variation with the turbulence strength (PVI in Fig. 2) was found [18].

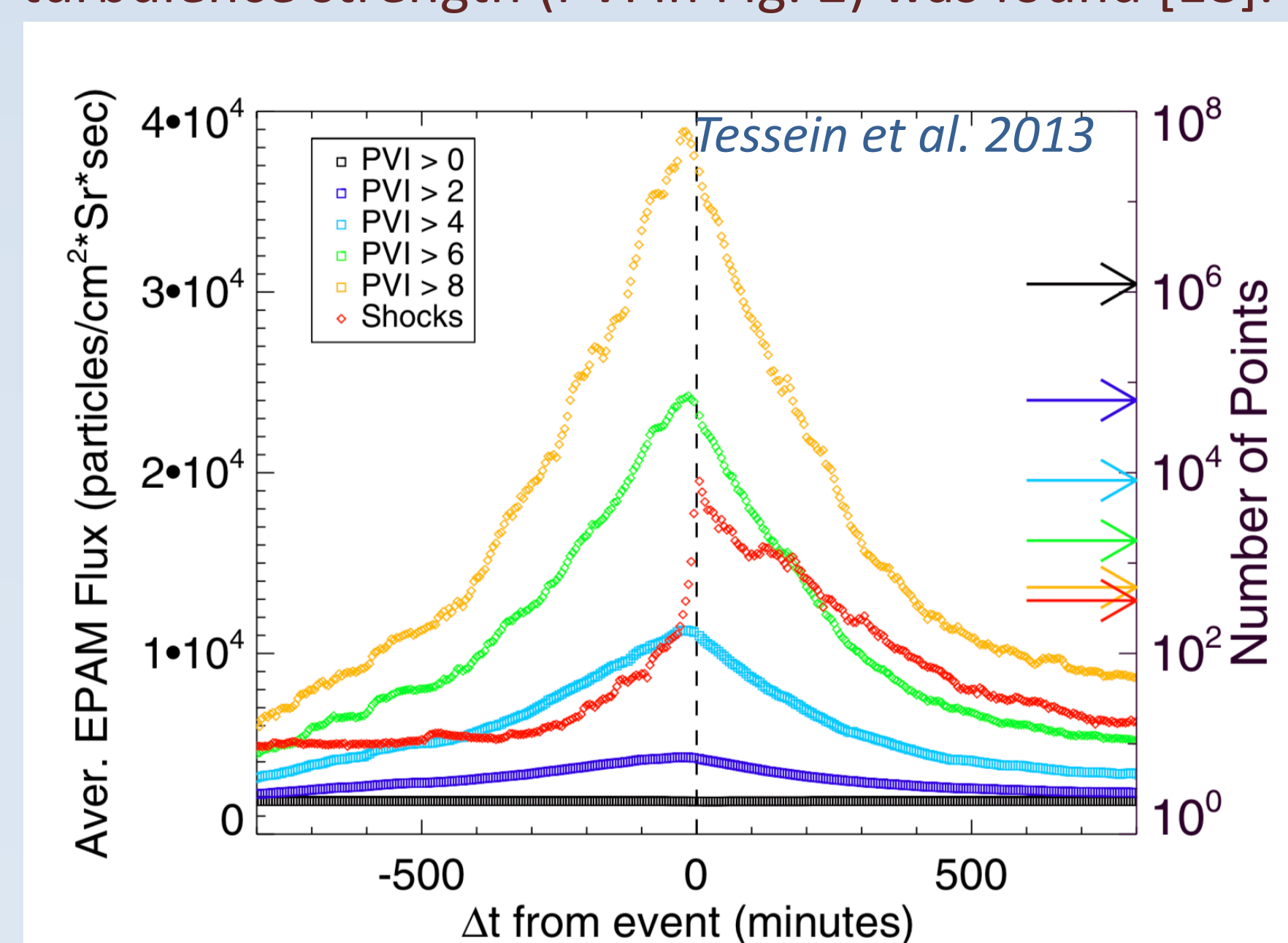


**FIGURE 2:** Variation of suprathermal tail fluxes (taken with ACE EPAM) across SW compressions for turbulence strength [18].

## Superposed Epoch Analysis of Suprathermal Tails

To address the raised question with good statistics Superposed Epoch Analysis (SPE) of compressions regions, as recently applied to the evolution of the pickup ion (PUI) cut-off using STEREO PLASTIC [19; Poster SH53C-3353], is used here. The evolution of the strongest 25% of all compressions (2007-14) is compiled in Fig. 3, with the tail normalized to the maximum PUI rate using 2 quiet time filters.

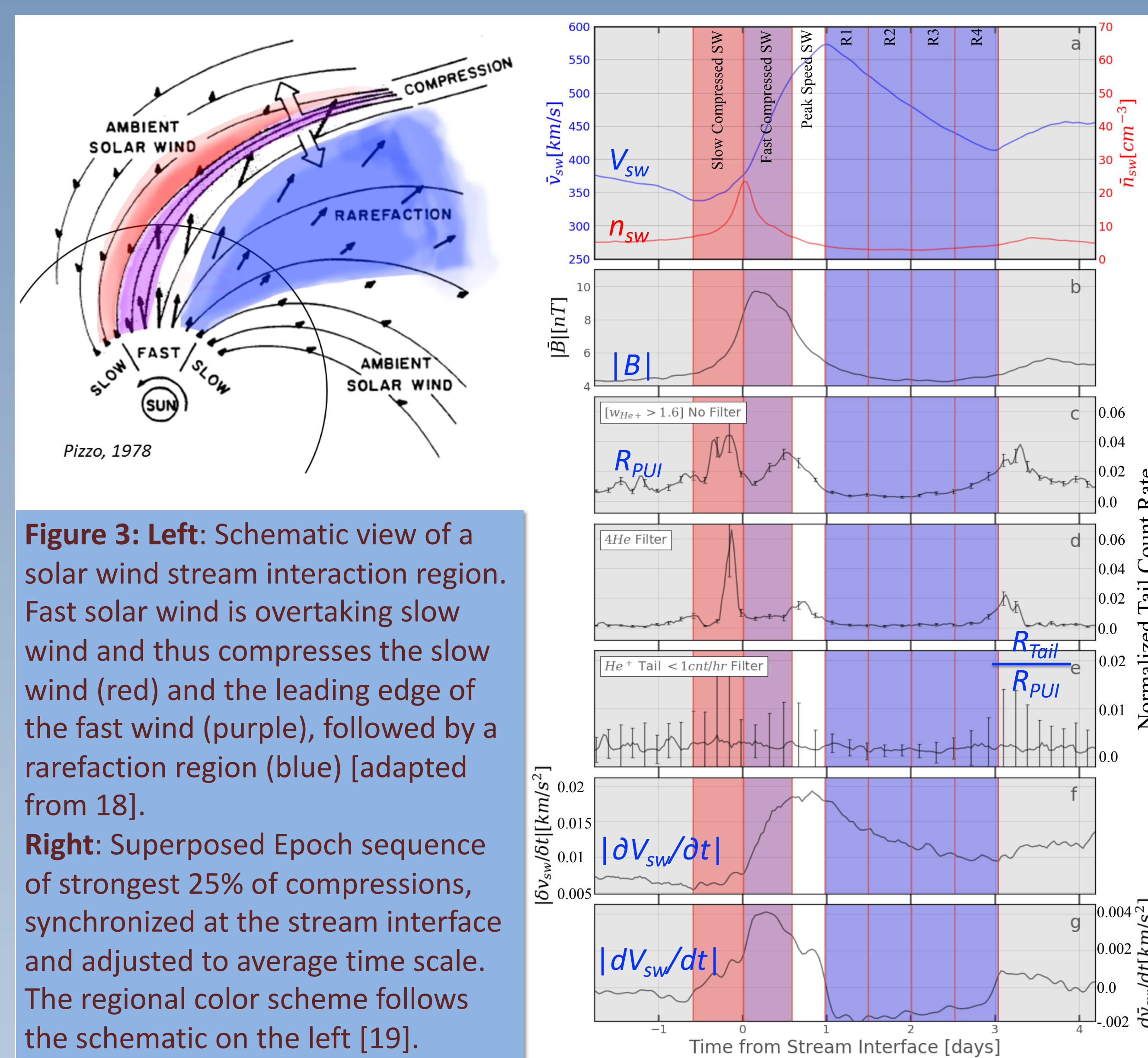


**Figure 3: Left:** Schematic view of a solar wind stream interaction region. Fast solar wind is overtaking slow wind and thus compresses the slow wind (red) and the leading edge of the fast wind (purple), followed by a rarefaction region (blue) [adapted from 18].

**Right:** Superposed Epoch sequence of strongest 25% of compressions, synchronized at the stream interface and adjusted to average time scale. The regional color scheme follows the schematic on the left [19].

## Effects of Quiet Time Selection Criteria

- He<sup>+</sup> tails appear strongest in the compressed SW, in Fig. 3 both in the slow and fast SW, where also the PUI rate is highest (Note: Tail rate normalized to PUI rate!) [19].
- No direct association with the strength of SW fluctuations ( $|\partial V_{sw}/\partial t|$ ) nor with the SW speed gradient ( $|dV_{sw}/dt|$ ) was found.
- Using a quiet time filter with STEREO SIT He fluxes at 0.16-0.24 MeV/nuc or no filter (not shown here), tail rates exhibit a minimum in the center of the rarefaction region [Mö 2019].
- Filtering with the PLASTIC He<sup>+</sup> rate as in [2], no variation of the tail rate is visible, yet randomly distributed “quiet time” accumulation time bins are identified even inside compressions, where mean rates are high.

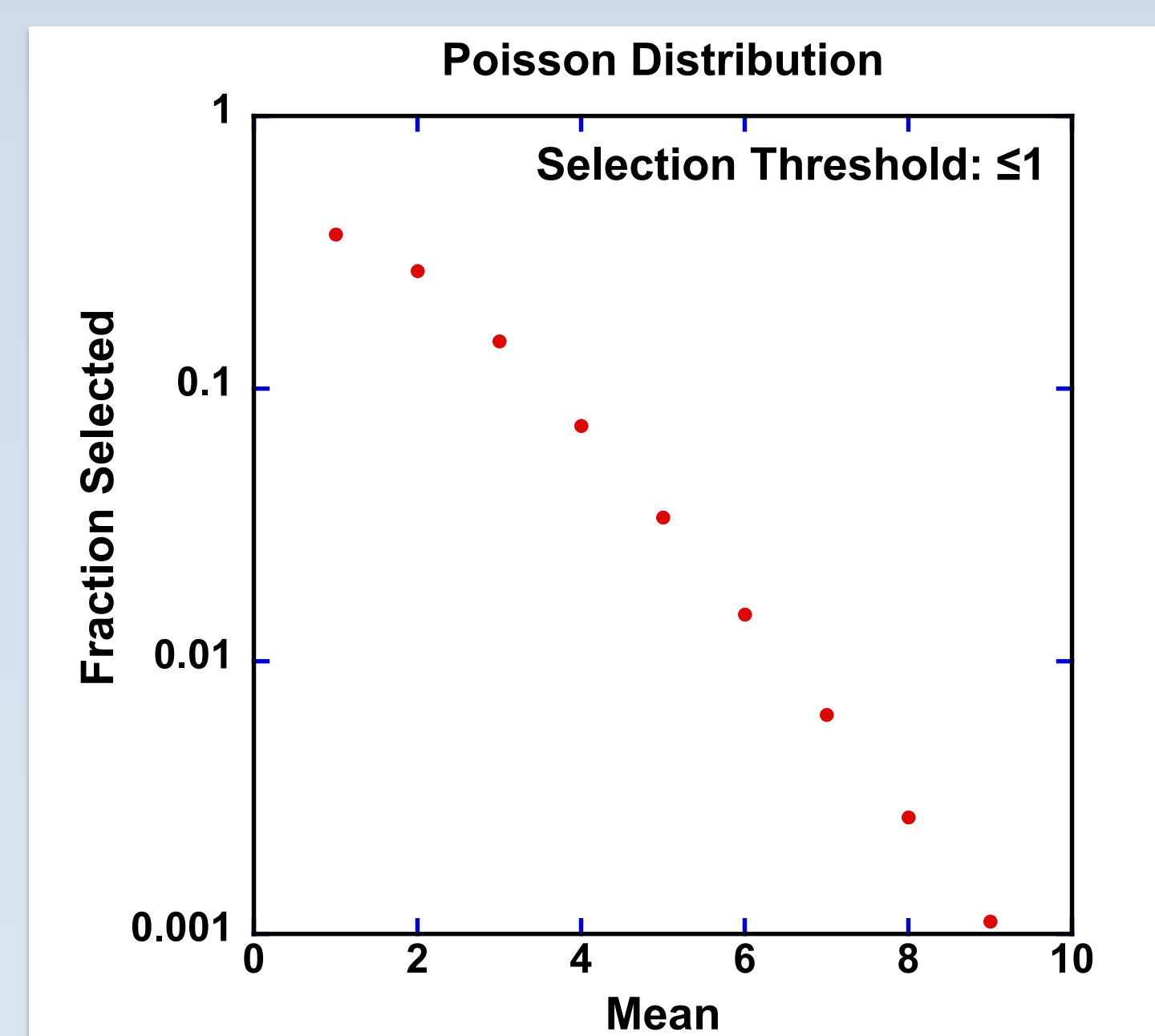


**FIGURE 4** Fraction of selected data time periods as a function of mean count rate for a threshold of  $\leq 1$  Ct/h, if the events are Poisson distributed [19]

This surprising finding of “quiet time” intervals for a rate threshold filter applied to the observed tail population as in [2] was interpreted as a result of He<sup>+</sup> counts distributed according to Poisson statistics, as demonstrated in Fig. 4. It shows the fractions of time intervals selected with  $\leq 1$  Count/interval as a function of the mean Count Rate.

This suggests a stochastic selection of “quiet time intervals” with the often-used Count Rate criterion [2]. What about the SW speed criterion [1, 3]?

## Variation of Tails Across Compression Regions

We have expanded our analysis by sub-dividing the complement of all compressions found with STEREO PLASTIC from 2007 through 2014 into sets with increasing SW speed gradients (proxy for compression strength), here with the SIT He<sup>+</sup> Filter (as in Fig. 3). The SW and IMF parameters are shown for the center SW speed gradient (81.5 km/s/day), while the Tail Fraction is shown for all gradient bins.

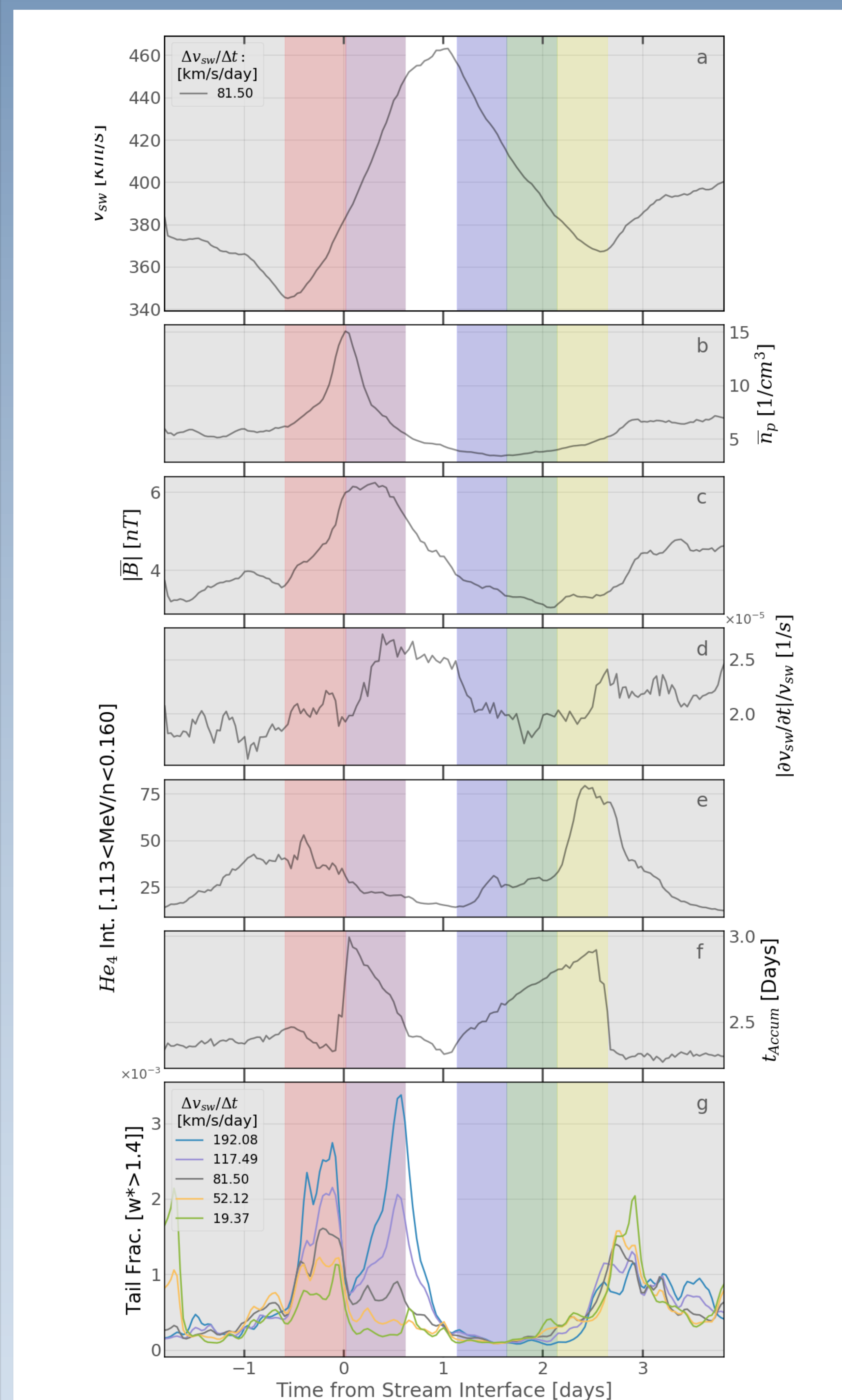


**FIGURE 5:** SPE accumulation of suprathermal tails and SW parameters, with time adjustment as in Figure 3. Panels a) SW speed  $V_{sw}$ , b) SW density  $n_{sw}$ , c) IMF  $B$ , d) SW speed fluctuations  $|\partial V_{sw}/\partial t|/V_{sw}$ , e) SIT He<sup>+</sup> (0.113-0.16 MeV/n), f) actual accumulation time  $t_{Accum}$  for compression gradient  $\Delta V_{sw}/\Delta t = 81.5 \pm 14$  km/s/day. Bottom panel g): Integral Tail PSD normalized to total PUI PSD for 5 compression gradient ranges, time scales adjusted to the one for  $\Delta V_{sw}/\Delta t = 81.5$  km/s/day.

## Main results from Fig. 5:

- Tail fluxes always strongest in the compressions and lowest in the center of the rarefaction, independent of compression strength. Peak after Rarefaction indicates arrival of next compression.
- Peak in SIT Energy Range falls before Tail Peak
- Two strongest compression ranges (117 and 192 km/s/day) show two distinct peaks, in the slow compressed SW and at the end of the fast compressed SW. This may be connected to the development of a forward shock in the slow SW and a reverse shock in the fast SW, where the most effective acceleration occurs.
- Again, no association with SW fluctuation level

## Variation of Suprathermal Tail Spectra

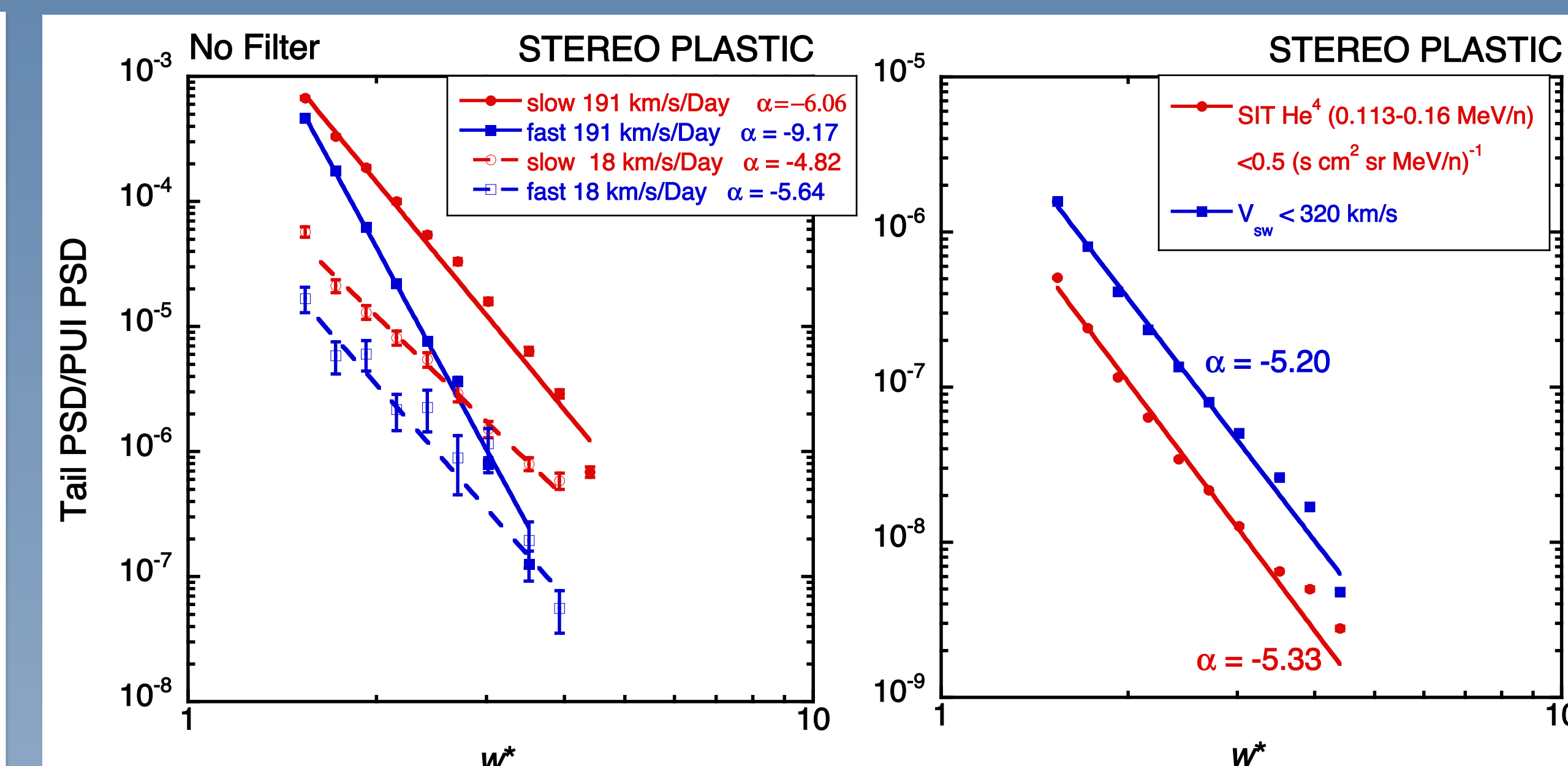


**FIGURE 6:** Suprathermal tail spectra as a function of speed  $w^*$  normalized to the SW speed in the SW frame, with the cut-off speed adjusted for the radial interstellar flow speed at 1 AU.

**Left:** SPE Spectra for Slow and Fast Compressed SW with SW speed gradient  $\Delta V_{sw}/\Delta t = 191$  and 18 km/s/Day

**Right:** Integrated tail spectra with SIT He<sup>+</sup> and  $V_{sw} < 320$  km/s filter applied.

- Tail spectra show a power law in the observed  $w^*$ -range, typically harder in the slow than in the fast compressed SW
- Tail spectra averaged over all regions, with SIT He<sup>+</sup> and  $V_{sw} < 320$  km/s quiet time filter applied, appear to follow approx.  $v^{-5}$
- Slowest SW provides strong tails, largely from slow compressed SW

## Conclusions & Outlook

- SPE Analysis of SW Compressions Indicates Clearly that Suprathermal Tails are Strongest in Compressions and Weakest in the Center of the Rarefaction Region Suggesting that Tail Populations May Stem from Compressions and Shocks and are Transported Everywhere Else
- There Appears to be a Trend in the Power Laws with Harder Spectra in the Slow Compressed SW Compared to the Fast SW, with Noticeable Variation in the Power Index
- Spectra Obtained from the Entire Compilation End Up Close to  $v^{-5}$  Suggesting a Superposition of Sources as Proposed in [22]
- To Test the Emerging Hypothesis that Suprathermal Tails may Arise from Localized Compressions and Shocks, be Transported into Rarefaction Regions, and Form a Superposition, Observations will be Combined with Simulations of the Acceleration and Transport Processes, Using the EPREM Simulation Framework [23]
- For Extended Continuous Observations and Cross-Calibration, STEREO PLASTIC Needs to be Operational into the IMAP Era

## References

- Gloeckler, G, et al. 2008 *AIP Conf. Proc.* **1039** 367
- Fisk, L A, & Gloeckler 2006 *Astrophys. J.* **640** L79
- Gloeckler, G, et al. 2000 *AIP Conf. Proc.* **528**, 221
- Desai, M I, et al. 2006 *Astrophys. J. Lett.* **645** L81
- Dayeh, M A, et al. 2017 *Astrophys. J.* **835** 155
- Fisk, L A, & Gloeckler 2008 *Astrophys. J.* **686** 1466
- Fisk, L A, & Gloeckler 2014 *J. Geophys. Res.* **119** 8773
- Jokipii, J R, & M A Lee 2010 *Astrophys. J.* **713** 475
- Zhang, M, 2010 *J. Geophys. Res.* **115** A12102
- Zhang, M, & M A Lee 2013 *Space Sci. Rev.* **176** 133
- Drake, J F, et al. 2012 *Astrophys. J.* **763** L5
- Zank, G P, et al. 2014 *Astrophys. J.* **797** 28
- Zhao, L-L, et al. 2018 *Astrophys. J. Lett.* **864** L34
- Giacalone, J, et al. 2002 *Astrophys. J.* **573** 845
- Richardson, I G, 2004 *Space Sci. Rev.* **111** 267
- Zank, G P, et al. 2000 *J. Geophys. Res.* **105** 25079
- Schwadron, N A, et al. 1996 *Geophys. Res. Lett.* **23** 2871
- Tessein, J A, et al. 2013 *Astrophys. J. Lett.* **776** L8
- Bower, J, et al. 2019 *J. Geophys. Res.* **124** 6418
- Pizzo, V, 1978 *J. Geophys. Res.* **83** 5563
- Möbius, E, et al. 2019 *IOP J. of Phys., Conf. Ser.* **1332** 012011
- Schwadron, N A, et al. 2010a *Astrophys. J.* **713** 1386
- Schwadron, N A, et al. 2010b *Space Weather* **8**